THE JOURNAL OF BIOLOGICAL CHEMISTRY
Vol. 279, No. 22, Issue of May 28, pp. 23193–23199, 2004
Printed in U.S.A.


# Role of ATP Hydrolysis in the Antirecombinase Function of *Saccharomyces cerevisiae* Srs2 Protein*

Received for publication, March 8, 2004
Published, JBC Papers in Press, March 27, 2004, DOI 10.1074/jbc.M402586200

**Lumir Krejci‡, Margaret Macris‡, Ying Li§, Stephen Van Komen‡, Jana Villemain¶, Thomas Ellenberger§, Hannah Klein‖, and Patrick Sung‡****

*From the ‡Department of Molecular Biophysics and Biochemistry, Yale University School of Medicine, New Haven, Connecticut 06520, the §Department of Biological Chemistry and Molecular Pharmacology, Harvard Medical School, Boston, Massachusetts 02115, the ¶Institute of Biotechnology and Department of Molecular Medicine, University of Texas Health Science Center at San Antonio, San Antonio, Texas 78245, and the ‖Department of Biochemistry, New York University School of Medicine, New York, New York 10016*

**Mutants of the *Saccharomyces cerevisiae SRS2* gene are hyperrecombinogenic and sensitive to genotoxic agents, and they exhibit a synthetic lethality with mutations that compromise DNA repair or other chromosomal processes. In addition, *srs2* mutants fail to adapt or recover from DNA damage checkpoint-imposed $G_2$/M arrest. These phenotypic consequences of ablating *SRS2* function are effectively overcome by deleting genes of the *RAD52* epistasis group that promote homologous recombination, implicating an untimely recombination as the underlying cause of the *srs2* mutant phenotypes. The *SRS2*-encoded protein has a single-stranded (ss) DNA-dependent ATPase activity, a DNA helicase activity, and an ability to disassemble the Rad51-ssDNA nucleoprotein filament, which is the key catalytic intermediate in Rad51-mediated recombination reactions. To address the role of ATP hydrolysis in Srs2 protein function, we have constructed two mutant variants that are altered in the Walker type A sequence involved in the binding and hydrolysis of ATP. The srs2 K41A and srs2 K41R mutant proteins are both devoid of ATPase and helicase activities and the ability to displace Rad51 from ssDNA. Accordingly, yeast strains harboring these *srs2* mutations are hyperrecombinogenic and sensitive to methylmethane sulfonate, and they become inviable upon introducing either the *sgs1*Δ or *rad54*Δ mutation. These results highlight the importance of the ATP hydrolysis-fueled DNA motor activity in *SRS2* functions.**

DNA helicases perform important functions in various chromosomal transactions, including replication, repair, recombination, and transcription (1, 2). These proteins utilize the chemical energy from the hydrolysis of a nucleoside triphosphate to dissociate DNA structures and nucleoprotein complexes. Interestingly, mutations in several DNA helicases are involved in the pathogenesis of human diseases. For instance, mutations in the XPB and XPD helicases, which constitute subunits of the transcription factor TFIIH that has a dual role in nucleotide excision repair, lead to the cancer prone syndrome xeroderma pigmentosum (3). Furthermore, mutations in the BLM, WRN, and RecQ4 proteins, members of the RecQ helicase family, cause the cancer-prone Bloom, Werner, and Rothmund-Thomson syndromes, respectively (4, 5).

We are interested in the biology of various DNA helicases that influence homologous recombination and DNA repair processes. One such helicase is encoded by the *Saccharomyces cerevisiae SRS2* gene, altered forms of which were first described as either suppressors of the DNA damage sensitivity of *rad6* and *rad18* mutants (6) or as hyperrecombination mutants (7). Detailed genetic analyses have shown that a major function of *SRS2* is to attenuate homologous recombination activity to allow for the channeling of certain DNA lesions into the *RAD6*/*RAD18*-mediated postreplication repair pathway (8, 9). Accordingly, *srs2* mutants are sensitive to DNA damaging agents and show a hyperrecombination phenotype. Genetic deletion of the *RAD51* or *RAD52*, key members of the *RAD52* epistasis group functioning in homologous recombination, alleviates the DNA damage sensitivity and hyperrecombination phenotypes of *srs2* mutants (8), implicating untimely recombination events as the progenitor of these *srs2* phenotypes. *Srs2* mutations are lethal when combined with mutations in a variety of genes needed for DNA repair and other chromosomal processes, *e.g.* with mutations in the DNA repair and recombination gene *RAD54* and also with mutations in *SGS1*, which codes for the sole RecQ helicase in *S. cerevisiae* (10, 11). The synthetic lethality encountered in the *srs2 sgs1* and *srs2 rad54* double mutants is suppressed by inactivating key recombination genes (11). The available genetic evidence therefore implicates Srs2 protein in the attenuation of recombination events that produce toxic DNA structures or nucleoprotein intermediates (12, 13).

In congruence with the genetic data, biochemical assays have shown that the Srs2 protein strongly suppresses the recombinase activity of Rad51. Interestingly, although Srs2 has the ability to unwind DNA (14, 15) and had been predicted to dissociate DNA intermediates in recombination reactions, its antirecombinase function can be attributed to an ability to disassemble the Rad51-single-stranded DNA (ssDNA)[1] nucleoprotein filament (14, 15), the key catalytic intermediate in recombination reactions (16). Likewise, the failure of *srs2* mu-

* This work was supported by National Institutes of Health Grants ES07061, GM57814, and GM53738, by Department of Energy Grant DE-FG02-01ER63071, by National Institutes of Health Postdoctoral Fellowship F32GM065746, and by Department of Defense Postdoctoral Fellowship BC020457. The molecular electron microscopy facility at Harvard Medical School was established by a donation from the Giovanni Armeise Harvard Center for Structural Biology and is maintained through a National Institutes of Health grant. The costs of publication of this article were defrayed in part by the payment of page charges. This article must therefore be hereby marked "*advertisement*" in accordance with 18 U.S.C. Section 1734 solely to indicate this fact.

** To whom correspondence should be addressed: Molecular Biophysics and Biochemistry, Yale University School of Medicine, 333 Cedar St., SHM C130A, New Haven, CT 06520. Tel.: 203-785-4553; Fax: 203-785-6037; E-mail: Patrick.Sung@yale.edu.

[1] The abbreviations used are: ssDNA, single-stranded DNA; MMS, methylmethane sulfonate; BSA, bovine serum albumin; dsDNA, double-stranded DNA; RPA, replicative protein A.

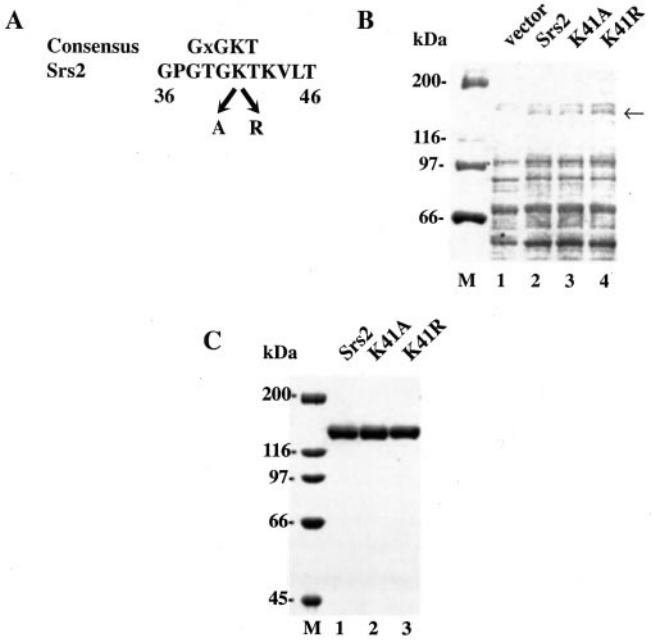


FIG. 1. **Expression and purification of srs2 K41A and srs2 K41R mutant proteins.** *A*, sequence of the Walker type A motif in Srs2 and the two mutant alleles, K41A (*A*) and K41R (*R*), constructed for this study. *B*, extracts from *E. coli* cells harboring the empty protein expression vector pET11c (*vector*, *lane 1*) and plasmids that express wild-type Srs2 (*lane 2*), srs2 K41A (*K41A*, *lane 3*) and srs2 K41R (*K41R*, *lane 4*) proteins were subjected to SDS-PAGE in a 7.5% gel and stained with Coomassie Blue. The *arrow* marks the position of the wild-type Srs2 and mutant srs2 proteins. *C*, purified Srs2 (*lane 1*), srs2 K41A (*K41A*, *lane 2*), and srs2 K41R (*K41R*, *lane 3*) proteins, 2 $\mu$g of each, were run in a 7.5% SDS-PAGE and then stained with Coomassie Blue.

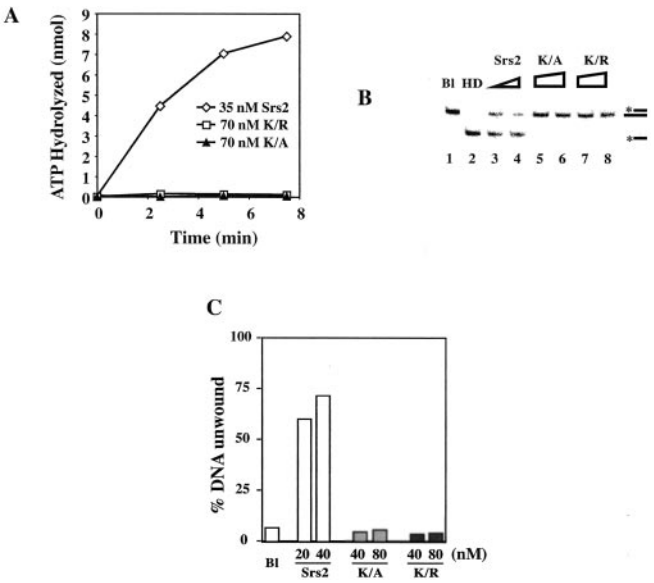


FIG. 2. **Biochemical properties of srs2 Walker mutants.** *A*, the ssDNA-dependent ATP hydrolysis activities of Srs2 (35 nM), srs2 K41A (*K/A*, 70 nM), and srs2 K41R (*K/R*, 70 nM) proteins were measured as described under "Materials and Methods." *B*, the DNA unwinding activities of Srs2 (20 and 40 nM in *lanes 3* and *4*), srs2 K41A (*K/A*, 40 and 80 nM in *lanes 5* and *6*), and srs2 K41R (*K/R*, 40 and 80 nM in *lanes 7* and *8*) proteins were assayed using a 3′-tailed DNA helicase substrate. The reaction mixtures were deproteinized and resolved in a native 12% polyacrylamide gel. *HD*, heat-denatured substrate; *Bl*, reaction mixture that did not contain any protein. *C*, quantification of the data in *B*.

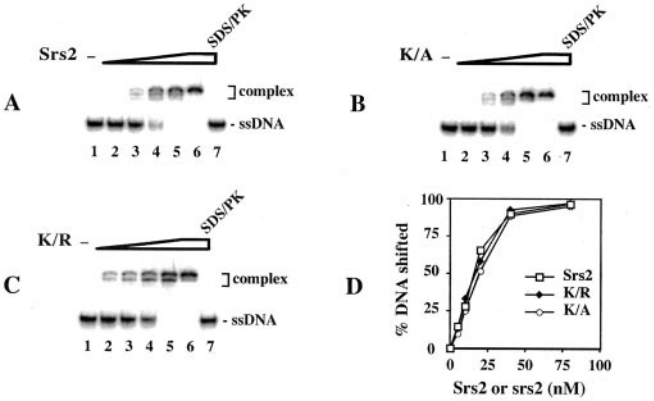


FIG. 3. **srs2 K41A and srs2 K41R proteins have normal DNA binding activity.** Increasing concentrations (5, 10, 20, 40, and 80 nM in *lanes 2–6*, respectively) of Srs2 (*A*), srs2 K41A (*K/A* in *B*), and srs2 K41R (*K/R* in *C*) were incubated with a $^{32}$P-labeled ssDNA oligonucleotide, and the reaction mixtures were analyzed in 12% native polyacrylamide gels. In *lane 7*, the highest concentration (80 nM) of Srs2 or srs2 mutant was incubated with the oligonucleotide substrate, but the reaction mixture was treated with SDS and proteinase K (*SDS/PK*) prior to gel analysis. In *lane 1*, the oligonucleotide substrate was incubated without protein. The percent DNA substrate shifted by Srs2, srs2 K41A, and srs2 K41R was determined by phosphorimaging analysis of the dried gels, and the data points are plotted in *D*.

tants to recover from or adapt to DNA damage checkpoint-imposed $G_2$/M cell cycle arrest has been linked to a failure to remove Rad51 from DNA (17). These results imply that, in addition to its ability to unwind double-stranded DNA, Srs2 has a motor activity that clears proteins from single-stranded DNA. Srs2 physically interacts with Rad51 in the yeast two-hybrid system and *in vitro* (14), and it has been suggested that complex formation between Srs2 and Rad51 helps target the former to DNA sites where Rad51 nucleoprotein filaments have assembled (14). In addition to the recombination-related phenotypes, the *srs2*Δ mutant is partially deficient in the activation of the intra-S DNA damage checkpoint in response to treatment with methylmethane sulfonate (MMS) (18). Additionally, two independent studies (19, 20) have implicated *SRS2* in DNA double-strand break repair by the synthesis-dependent single-strand annealing mechanism as well. Srs2 also appears to influence the efficiency of single-strand annealing (17).

As summarized above, Srs2 appears to have a multifunctional role in nuclear processes including an ability to unwind DNA and disassemble the Rad51-ssDNA nucleoprotein filament. Here, we address the role of ATP in Srs2 protein functions by mutating the highly conserved lysine residue in the Walker type A motif expected to be involved in ATP binding and hydrolysis. We show that the resulting srs2 K41A and srs2 K41R mutant proteins are devoid of ATPase and helicase activities and are unable to dislodge Rad51 from DNA. Genetic analyses reveal that the *srs2 K41A* and *srs2 K41R* mutations cause hyperrecombination, sensitivity to MMS, and synthetic lethality with the *sgs1*Δ or *rad54*Δ mutation. Our results thus reveal a requirement for the Srs2 DNA motor activity in recombination attenuation. However, the *srs2 K41A* and *srs2 K41R* mutants are less sensitive to MMS than *srs2* null cells and exhibit a more pronounced hyperrecombinational phenotype than the latter. It therefore seems possible that Srs2 has additional functions that are not strictly linked to ATP hydrolysis and Rad51 removal from DNA.

## MATERIALS AND METHODS

*Yeast Media and Strains*—Yeast extract-peptone-dextrose (YPD) medium, synthetic complete (SC) medium, and synthetic complete media without leucine (SC-Leu), without uracil (SC-Ura), and without leucine and uracil (SC-Leu-Ura) were prepared as described (21). Media containing 5-fluoro-orotic acid were prepared as described (21). Except where noted, all strains are *RAD5* derivatives of W303 (22). The re-

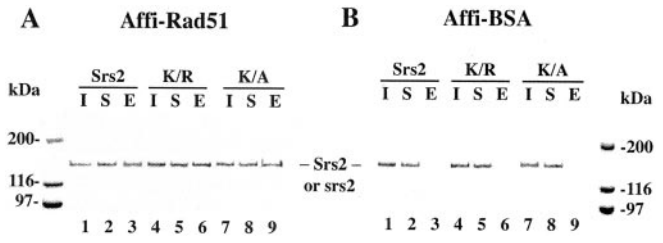


FIG. 4. **Interaction of mutant srs2 proteins with Rad51.** Srs2, srs2 K41A (*K/A*), and srs2 K41R (*K/R*) proteins were mixed with Affi-Rad51 beads (*A*) and Affi-BSA beads (*B*). The starting material (*I*), supernatant that contained unbound Srs2, srs2 K41A, or srs2 K41R (*S*), and the SDS eluate (*E*) were resolved by SDS-PAGE in a 10% gel and then stained with Coomassie Blue.

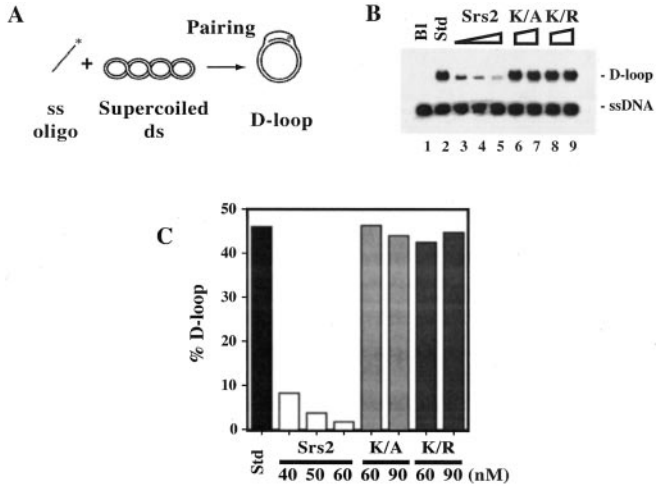


FIG. 5. **Mutant srs2 proteins fail to attenuate Rad51/Rad54/RPA-mediated D-loop reaction.** *A*, D-loop reaction scheme. The radiolabeled 90-mer oligonucleotide D1 is paired with homologous pBluescript form I DNA to yield a D-loop. *B*, in *lanes 2–9*, radiolabeled D1 was incubated with Rad51, Rad54, RPA, and with or without Srs2 (40, 50, and 60 nM in *lanes 3–5*), srs2 K41A (*K/A*, 60 and 90 nM in *lanes 6* and *7*), or srs2 K41R (*K/R*, 60 and 90 nM in *lanes 8* and *9*) and then pBluescript form I DNA was incorporated. The reaction (*lane 2*) without Srs2 or mutant srs2 is designated as *Std*. *Lane 1* contained the DNA substrates but no protein (*Bl*). The reaction mixtures were incubated for 4 min, deproteinized, and then subject to electrophoresis in a 1% agarose gel. The gel was dried and analyzed in the PhosphorImager. *C*, the data points from phosphorimaging analysis of the gel in *B* are plotted.

maining strains were derived from HKY344-27C and carry *leu2-112*::*URA3*::*leu2-k* and *his3-513*::*TRP1*::*his3-537* recombination reporters (7).

*Plasmid Construction*—To generate the *SRS2*::pUC18 plasmid, the ORF of *SRS2* was amplified using the following primers: C*GGGATC*CACATATGTCGTCGAACAATGATCTTTGGTTGC (sense, BamHI site italic, NdeI underline) and CG*GGATCC*GGAATTCCCTACTAATCGATGACTATGATTTCACCG (antisense, BamHI site italic, EcoRI site underline). The PCR product was digested with BamHI and ligated into the BamHI-digested pUC18. The mutations in the Walker A site in Srs2, K41A, and K41R, were introduced by using mutagenic DNA primers and QuikChange site-directed mutagenesis kit (Stratagene). The mutations were confirmed by DNA sequencing. For protein purification, the *srs2 K41R* and *srs2 K41A* mutant genes were introduced into the pET11c vector. pBS::SRS2 and YIpLac211-srs2 were constructed as follows. The 3.1-kb NdeI-BglII fragments containing the K41R or K41A segments of the mutated *SRS2* gene were used to replace the wild-type *SRS2* segment in plasmid pRL101 (9). Next, a 6.4-kb EcoRI-SalI fragment containing all of the *SRS2* coding region plus 927 bp upstream of the ATG start codon and 1602 bp downstream of the stop codon was inserted into the EcoRI and SalI sites of the polylinker of YIpLac211, which carries the *URA3* selectable marker, to form pHK284 (*srs2 K41A*) and pHK286 (*srs2 K41R*). These plasmids were linearized with BglII and then used to transform W303 and HKY344–27C strains. After selecting for Ura$^+$ transformants, cells were grown non-selectively and

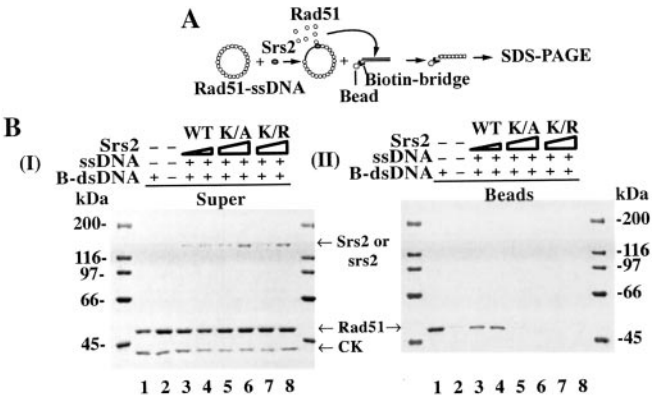


FIG. 6. **Disassembly of Rad51-ssDNA nucleoprotein filaments is coupled to ATP hydrolysis by Srs2.** *A*, Rad51 molecules displaced by Srs2 can be trapped on immobilized DNA duplex attached to streptavidin magnetic beads. Rad51 associated with the magnetic bead-bound duplex is eluted by SDS followed by SDS-PAGE analysis. *B*, pre-assembled Rad51-ssDNA nucleoprotein filaments (*lanes 2–8*) were incubated with Srs2 (*WT*, 60 and 90 nM in *lanes 3* and *4*), srs2 K41A (*K/A*, 90 and 180 nM in *lanes 5* and *6*), or srs2 K41R (*K/R*, 90 and 180 nM in *lanes 7* and *8*), and the reaction mixtures mixed with streptavidin magnetic beads containing biotinylated dsDNA (*lanes 3–8*). In *lane 1*, free Rad51 was mixed with streptavidin magnetic beads that contained biotinylated dsDNA, and in *lane 2*, free Rad51 was mixed with streptavidin magnetic beads that did not contain any dsDNA. The supernatant (*Super*, *panel I*) and bead-bound (*Beads*, *panel II*) fractions were subjected to SDS-PAGE in a 7.5% gel and stained with Coomassie Blue. *CK* denotes creatine kinase in the buffer.

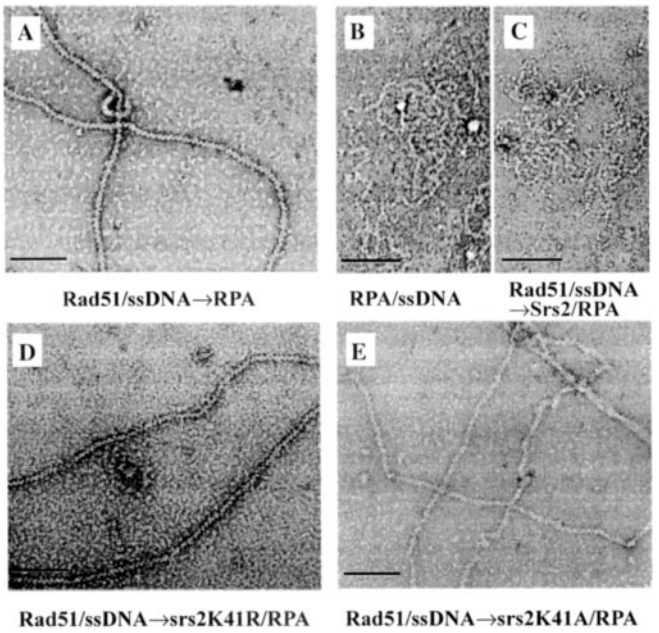


FIG. 7. **Electron micrographs showing effects of Srs2 and mutant srs2 proteins on Rad51-ssDNA filaments.** *A*, Rad51 was incubated with ssDNA before RPA was added, and an example of the resulting Rad51-ssDNA nucleoprotein filaments is shown. *B*, RPA was incubated with ssDNA, and an example of the RPA-ssDNA nucleoprotein complex that formed is shown. *C*, incubation of preformed Rad51-ssDNA nucleoprotein filaments with Srs2 caused the displacement of Rad51 from DNA and the formation of RPA-ssDNA nucleoprotein complexes, an example of which is shown. *D* and *E*, srs2 K41R and srs2 K41A were incapable of disrupting the Rad51-ssDNA nucleoprotein filaments. The *dark bar* represents 100 nm.

then streaked on 5-fluoro-orotic acid plates. Fluoro-orotic acid-resistant colonies were tested for MMS sensitivity. MMS-sensitive colonies were examined for the presence of the *srs2* mutations by PCR amplification of the genomic region surrounding the *SRS2 K41* site. Primers used were CTTTTTCTTTTGCGCTGTAT and TCCCGAACTAAAGAAGGTGC. The mutant *srs2 K41A* and *K41R* sites carry an adjacent StyI

TABLE I
*Gene conversion in srs2 K41A and srs2 K41R strains*

Strains used for the gene conversion tests are derived from HKY344-27C and are of the genotype *leu2-112*::*URA3*::*leu2-k his3-513*::*TRP1*::*his3-537 ura3-52 trp1 ade1-101*. Strains used are HKY344-27C, HKY344-109D, and HKY1355-7B for *SRS2*, HKY1355-8B, HKY1355-12C, and HKY1355-16C for *srs2 K41A*, HKY1439-5C, HKY1439-9C, and HKY1439-10A for *srs2 K41R*, and F103-2A56, F126-1C, and F121-8C for *srs2*Δ.

| Genotype | Leu + Ura + rate | Increase | His + Trp + rate | Increase |
|---|---|---|---|---|
| | | *-fold* | | *-fold* |
| *SRS2* | $5.65 \times 10^{-6} \pm 1.24 \times 10^{-6}$ | | $3.92 \times 10^{-6} \pm 1.65 \times 10^{-6}$ | |
| *srs2 K41A* | $5.22 \times 10^{-5} \pm 3.63 \times 10^{-5}$ | 9.24 | $6.15 \times 10^{-5} \pm 1.14 \times 10^{-5}$ | 15.69 |
| *srs2 K41R* | $6.96 \times 10^{-5} \pm 3.75 \times 10^{-5}$ | 12.32 | $6.77 \times 10^{-5} \pm 3.11 \times 10^{-5}$ | 17.27 |
| *srs2*Δ | $1.93 \times 10^{-5} \pm 3.06 \times 10^{-6}$ | 3.42 | Not done | |

site that is not present in the wild-type sequence. PCR products were tested for the StyI site by restriction digestion and agarose gel electrophoresis.

*Srs2 Expression and Purification*—srs2 K41A and srs2 K41R proteins were overexpressed in *Escherichia coli* cells and purified to near homogeneity as described previously for wild-type Srs2 (14, 23). Rad51 was overexpressed in yeast and purified to near homogeneity as described (16). The concentration of the wild-type Srs2 and mutant srs2 proteins was determined by densitometric scanning of SDS-polyacrylamide gels containing multiple loadings of purified proteins against known quantities of bovine serum albumin. The concentrations of Rad51 and RPA were determined using extinction coefficients of $1.29 \times 10^4$ and $8.8 \times 10^4$ at 280 nm, respectively (24).

*DNA Substrates*—The H2 and D1 oligonucleotides used in the construction of the helicase substrate have been described (23). Oligo-1 used in the DNA binding experiments has also been described (25). The oligonucleotides were purified from 12% polyacrylamide gels and 5′-end-labeled with [$\gamma$-$^{32}$P] ATP using T4 polynucleotide kinase. The unincorporated nucleotide was removed from the oligonucleotides using Spin30 columns (Bio-Rad). The DNA helicase substrate was obtained by heating equimolar amounts of H2 and radiolabeled D1 oligonucleotides to 95 °C for 10 min in buffer B (50 mM Tris-HCl, pH 7.5, 10 mM $MgCl_2$, 100 mM NaCl), followed by slow cooling to room temperature. The annealed substrate was purified from a 12% non-denaturing polyacrylamide gel, as described (23). The $\phi$X174 (+) strand was purchased from New England Biolabs.

*ATPase Assay*—Srs2 (35 nM) was incubated with viral ssDNA (25 $\mu$M nucleotides) in 10 $\mu$l of buffer A (30 mM Tris-HCl, pH 7.2, 2.5 mM $MgCl_2$, 1 mM dithiothreitol, 150 mM KCl, and 100 $\mu$g/ml BSA) and 1 mM [$\gamma$-$^{32}$P] ATP for the indicated times at 37 °C. The released phosphate was separated from unhydrolyzed ATP by thin layer chromatography, as described (26). The levels of hydrolysis were determined by phosphorimaging analysis of the thin layer chromatography plates in a Personal Molecular Imager FX (Bio-Rad).

*DNA Helicase Assay*—Srs2 (20 and 40 nM), srs2 K41R (40 and 80 nM), or srs2 K41A (40 and 80 nM) was incubated at 30 °C for 5 min with the helicase substrate (300 nM nucleotides) in 10 $\mu$l of buffer H (30 mM Tris-HCl, pH 7.5, 2.5 mM $MgCl_2$, 1 mM dithiothreitol, 100 mM KCl, 2 mM ATP, and 100 $\mu$g/ml BSA). The reaction mixtures were resolved by electrophoresis in a 12% non-denaturing polyacrylamide gel run in TAE buffer (40 mM Tris-HCl, pH 7.4, 0.5 mM EDTA) at 4 °C. The gel was dried onto Whatman DE81 paper and analyzed in the PhosphorImager.

*DNA Mobility Shift*—Varying amounts of Srs2, srs2 K41A or srs2 K41R (0–80 nM) was incubated with $^{32}$P-labeled oligo-1 (1.36 $\mu$M nucleotides) at 37 °C in 10 $\mu$l of buffer D (40 mM Tris-HCl, pH 7.8, 50 mM KCl, 1 mM dithiothreitol, and 100 $\mu$g/ml BSA) for 10 min. After the addition of gel loading buffer (50% glycerol, 20 mM Tris-HCl, pH 7.4, 2 mM EDTA, 0.05% orange G), the reaction mixtures were resolved in 12% native polyacrylamide gels in TAE buffer (40 mM Tris acetate, 1 mM EDTA) at 4 °C, and the DNA species were quantified using Quantity One software (Bio-Rad). To release the DNA substrate from bound Srs2 and srs2 mutants, the reaction mixtures were treated with 0.5% SDS and 0.5 mg/ml proteinase K at 37 °C for 10 min before being subject to electrophoresis.

*Binding of Srs2 to Rad51 Affi-beads*—Affi-gel 15 beads containing Rad51 (Affi-Rad51; 5 mg/ml) and bovine serum albumin (Affi-BSA, 12 mg/ml) were prepared as described previously (26). Purified Srs2, srs2 K41A, or srs2 K41R, 5 $\mu$g of each, was mixed with 5 $\mu$l of Affi-Rad51 or Affi-BSA in 60 $\mu$l of phosphate-buffered saline (10 mM $Na_2HPO_4$, 1.8 mM $KH_2PO_4$, pH 7.4, and 150 mM NaCl) for 30 min on ice. The beads were washed twice with 150 $\mu$l of the same buffer before being treated with 25 $\mu$l of 2% SDS to elute bound protein. The starting material, a supernatant that contained unbound Srs2, srs2 K41A, or srs2 K41R, and the SDS eluate, 10 $\mu$l of each, were analyzed by 10% SDS-PAGE and staining with Coomassie Blue.

TABLE II
*Mutation rates in srs2 K41A and srs2 K41R strains*

Strains used for the *CAN1* mutation rate determinations are derived from *CAN1* versions of W303 and are of the genotype *leu2-3, 112 his3-11, 15 ADE2 ura3-1 trp1-1 RAD5 CAN1*. Strains used are HKY1025-47D for *SRS2*, HKY1434-4A for *srs2 K41A*, HKY1433-8A for *srs2 K41R*, and HKY1303-1B for *srs2*Δ.

| Genotype | Can$^r$ rate | Increase |
|---|---|---|
| | | *-fold* |
| *SRS2* | $9.30 \times 10^{-8}$ | |
| *srs2 K41A* | $9.33 \times 10^{-8}$ | 1.0 |
| *srs2 K41R* | $4.66 \times 10^{-8}$ | 0.5 |
| *srs2*Δ | $1.41 \times 10^{-7}$ | 1.5 |

*D-loop Reaction*—The reactions were carried out in Buffer R (35 mM Tris-HCl, pH 7.4, 2.0 mM ATP, 2.5 mM $MgCl_2$, 50 mM KCl, 1 mM dithiothreitol, containing an ATP-regenerating system consisting of 20 mM creatine phosphate, 20 $\mu$g/ml creatine kinase) and had a final volume of 12.5 $\mu$l. The radiolabeled oligonucleotide D1 (3 $\mu$M nucleotides) was incubated with Rad51 (1 $\mu$M) for 5 min at 37 °C to assemble Rad51-ssDNA nucleoprotein filaments, followed by the incorporation of Rad54 (150 nM) and RPA (200 nM) and a 2 min incubation at 23 °C. The D-loop reaction was initiated by the addition of pBluescript replicative form I DNA (50 $\mu$M base pairs). The reaction mixtures were incubated at 30 °C for 4 min, deproteinized by treatment with SDS (0.5%) and proteinase K (0.5 mg/ml) at 37 °C for 10 min, and then run in a 1% agarose gel in TAE buffer. The gel was dried and subject to phosphorimaging analysis. The percentage D-loop refers to the quantity of the replicative form I substrate that had been converted into D-loop. When present, Srs2 (40, 50, and 60 nM), srs2 K41A (60 and 90 nM), and srs2 K41R (60 and 90 nM) were added to the pre-assembled Rad51-ssDNA nucleoprotein filaments, followed by a 4-min incubation at 37 °C before Rad54 and RPA were incorporated.

*Transfer of Rad51 to Bead-bound Biotinylated dsDNA*—M13mp18 circular (+) strand (7.2 $\mu$M nucleotides) was incubated for 5 min with Rad51 (2.4 $\mu$M) at 37 °C, followed by the addition of Srs2 (60 and 90 nM), srs2 K41A (90 and 180 nM), or srs2 K41R (90 and 180 nM) in a final volume of 20 $\mu$l of buffer R containing 0.01% igepal. After 3 min at 37 °C, 4 $\mu$l of magnetic beads containing dsDNA (14) were added to the reaction mixture, followed by constant mixing for 5 min at 23 °C. The beads were captured with the Magnetic Particle Separator (Roche Molecular Biochemicals), washed twice with the same buffer, and the bound Rad51 was eluted with 20 $\mu$l of 1% SDS. The supernatant, which contained unbound Rad51, and the SDS eluate (10 $\mu$l of each) were analyzed by SDS-PAGE.

*Electron Microscopy*—The reactions were carried out in buffer R and had a final volume of 12.5 $\mu$l. To assemble the Rad51 presynaptic filament, M13mp18(+) strand (7.2 $\mu$M nucleotides) and Rad51 (2.4 $\mu$M) were incubated at 37 °C for 5 min, followed by the addition of RPA (350 nM) and a 3 min incubation. To test the effects of Srs2 and mutant srs2 proteins, 60 nM of these proteins were incubated with the pre-assembled Rad51-ssDNA nucleoprotein filaments at 37 °C for 3 min. For electron microscopy, 2.5 $\mu$l of each reaction mixture was applied to copper grids coated with thin carbon film, after glow-discharging the grids for 2 min. The grids were washed twice with buffer R and stained for 30 s with 0.75% uranyl formate. After air-drying, the grids were examined with a Philips Tecnai 12 electron microscope under low-dose conditions. Images were recorded with a charge-coupled device camera (Gatan).

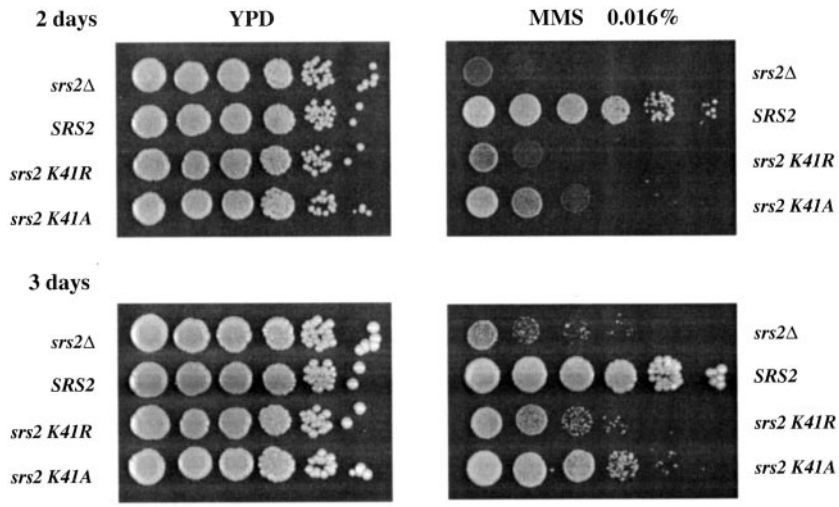


FIG. 8. **MMS sensitivity of the *srs2 K41A* and *srs2 K41R* mutants.** srs2 mutant strains grow normally on YPD plates but are sensitive when grown on plates containing MMS. Overnight cultures were serially diluted, and 3-μl aliquots were dropped on the plates. The pictures were taken after two and three days of incubation at 30 °C.

*Genetic Studies*—MMS sensitivity was determined using freshly made YPD plates containing 0.016% MMS. Overnight cultures of strains to be tested were serially diluted, and 3-μl aliquots of each dilution were applied onto YPD and YPD+MMS plates. Growth was assessed after 2 and 3 days at 30 °C. Forward mutation rates of *CAN1* were determined in haploid *CAN1* strains by fluctuation tests. These tests were conducted according to the median method (27) and were repeated three to five times for each genotype. Gene conversion between intrachromosomal *leu2-112* and *leu2-k* as well as between *his3-513* and *his3-537* heteroalleles was measured in haploid strain HKY344-27C and its isogenic derivatives.

## RESULTS

*srs2 Variants Mutated for the Walker Type A ATP Binding Motif*—Srs2 contains canonical Walker-type ATP binding motifs. For addressing the role of ATP binding and hydrolysis in Srs2 functions, we have substituted the highly conserved lysine residue (lysine 41) in the Walker type A motif with either alanine or arginine using site-directed mutagenesis (Fig. 1*A*). The *srs2 K41A* and *srs2 K41R* mutant genes were sequenced to ensure that no unintended change had been introduced during the mutagenesis procedure. To express the srs2 K41A and srs2 K41R proteins, the mutant genes were placed under the isopropyl-1-thio-β-D-galactopyranoside-inducible T7 promoter in the *E. coli* expression vector pET11c, which we previously used for the expression and purification of wild-type Srs2 (14). Expression of the srs2 K41A and srs2 K41R mutant proteins in *E. coli* was verified by SDS-PAGE analysis of cell extracts (Fig. 1*B*) and by immunoblot analysis of these extracts with affinity-purified anti-Srs2 polyclonal antibodies (14). The srs2 K41A and srs2 K41R mutant proteins were purified to near homogeneity (Fig. 1*C*) using the chromatographic procedure that we have developed for wild-type Srs2 (14).

*Biochemical Properties of srs2 K41A and srs2 K41R Mutant Proteins*—Based on studies with the equivalent Walker mutations in other DNA-dependent ATPases (28, 29), the srs2 K41A and srs2 K41R mutant proteins were expected to be defective in ATP hydrolysis. This expectation was confirmed by examining the ATPase activity of purified proteins with [α-$^{32}$P] ATP and thin layer chromatography (14, 23). We showed previously that ATP hydrolysis by Srs2 occurs only in the presence of DNA with ssDNA being much more effective than dsDNA in this regard (9, 23). As summarized in Fig. 2*A*, although robust ATPase activity was observed with wild-type Srs2 in the presence of ssDNA (14, 23), the two srs2 mutant proteins showed less than 1% of the wild-type level of ATP hydrolysis. Likewise, no significant ATP hydrolysis by either of the srs2 mutants was seen when the ssDNA was omitted or substituted with dsDNA (data not shown). We next examined the two srs2 mutant proteins for DNA helicase activity using a $^{32}$P-labeled substrate that contained a 40-bp duplex region adjacent to a 40-nucleotide 3′-ssDNA overhang (Fig. 2*B* and Ref. 23). As shown in Fig. 2*B*, although wild-type Srs2 at 40 nM unwound greater than 70% of the substrate after 5 min of incubation, neither of the srs2 mutants, even at the increased concentration of 80 nM, showed a significant helicase activity under the same conditions (Fig. 2*B*) or even after a prolonged incubation (data not shown).

Even though the results presented in Fig. 2 were consistent with the premise that the K41A and K41R mutations abolish the ATPase activity of Srs2, there existed the possible caveat that this defect had originated from a loss of DNA binding by the mutant proteins. For this reason, we compared the DNA binding ability of the two Walker mutants to that of the wild-type protein by a DNA mobility shift assay. To do this, increasing amounts of wild-type Srs2 and the two mutant proteins were incubated with a $^{32}$P-labeled 83-mer oligonucleotide, followed by resolution of the reaction mixtures in non-denaturing polyacrylamide gels and phosphorimaging analysis of the dried gels to detect and quantify the DNA mobility shift. As shown in Fig. 3, both srs2 mutant proteins were just as proficient as wild-type Srs2 in DNA binding. Consistent with this result, using the same DNA substrate, we found that DNA binding by wild-type Srs2 and the two srs2 mutant proteins is not influenced by ATP (data not shown).

*Attenuation of Rad51-mediated Homologous DNA Pairing and Strand Exchange by Srs2 Requires ATP Hydrolysis*—Recently, we (14) and Fabre and co-workers (15) demonstrated that Srs2 is highly adept at attenuating Rad51-mediated homologous DNA pairing and strand exchange, the biochemical reaction that serves to link recombining chromosomes (30). In addition, a physical interaction between Rad51 and Srs2 was demonstrated by us (14). Before examining the srs2 K41A and srs2 K41R mutant proteins for their ability to suppress the Rad51 recombinase activity, we first verified that the srs2 mutant proteins retain the ability to interact with Rad51. For this, purified Srs2, srs2 K41A, and srs2 K41R proteins were each mixed with Affi-Gel beads that contained covalently conjugated Rad51 protein (Affi-Rad51) or Affi-Gel beads that contained conjugated bovine serum albumin (Affi-BSA). After being washed with buffer, the Affi-Rad51 and Affi-BSA beads were treated with SDS to elute bound Srs2 and srs2 mutant proteins. As shown in Fig. 4*A*, the two srs2 mutant proteins interacted with Rad51 just as avidly as wild-type Srs2 did. As expected, neither the wild-type Srs2 protein nor either of the srs2 mutants was retained on the Affi-BSA control beads (Fig. 4*B*).

We employed the D-loop assay (Fig. 5*A*) for testing the proficiency of the srs2 K41A and srs2 K41R mutant proteins in recombination attenuation. As reported in our published work, the addition of a catalytic quantity of Srs2 (40–60 nM) to the D-loop reaction containing Rad51 (1 $\mu$M), Rad54 (150 nM), and RPA (200 nM) caused pronounced inhibition (Fig. 5, *B* and *C*). For instance, at 50 nM Srs2, the level of D-loop was suppressed by greater than 10-fold (Fig. 5, *B* and *C*). Importantly, as much as 90 nM of srs2 K41A and srs2 K41R did not exert any inhibitory effect on the D-loop reaction (Fig. 5, *B* and *C*), thus revealing a requirement for the Srs2 ATPase activity in the attenuation of the Rad51 recombinase activity. We independently verified this conclusion by using a homologous DNA pairing and strand exchange system that employs $\phi$X174 (+) strand DNA and linear duplex as substrates (Refs. 14 and 16, data not shown).

*Disassembly of Rad51-ssDNA Nucleoprotein Filament by Srs2 Requires ATP Hydrolysis*—The results above have verified that the ATPase activity of Srs2 protein is indispensable for attenuating Rad51-mediated recombination reactions *in vitro*. We have devised previously a bead-based biochemical assay to monitor the Srs2-mediated dissociation of Rad51 from ssDNA. Briefly, Rad51 molecules displaced by Srs2 from the presynaptic filament are trapped on a biotinylated duplex DNA fragment tethered to streptavidin-conjugated magnetic beads, followed by elution of Rad51 from the beads and SDS-PAGE analysis (Fig. 6*A*, and Ref. 14). As reported previously, incubation of Rad51 nucleoprotein filaments with Srs2 protein (60–90 nM) resulted in the release of Rad51 from the filaments as indicated by Rad51 being trapped on the streptavidin-magnetic beads that contained duplex DNA (Fig. 6*B*). Importantly, neither of the srs2 mutants, even in an amount twice that of Srs2 (180 nM), was capable of releasing Rad51 protein from the nucleoprotein filaments (Fig. 6*B*).

We also used electron microscopy to examine the ability of the two srs2 mutant proteins to catalyze the disassembly of the presynaptic filament, following the guidelines described in Krejci *et al.* (14). Briefly, the Rad51 presynaptic filament, which is extended and has a striated appearance (Fig. 7*A*), was incubated with Srs2 or the srs2 mutant proteins in the presence of RPA, and the dissociation of the Rad51 filament was gauged by the disappearance of the filament and the concomitant appearance of RPA-ssDNA nucleoprotein complexes, which appear as compact structures with bulges of bound protein molecules (14) (Fig. 7*B*). As expected, incubation of the Rad51 presynaptic filament with Srs2 led to its replacement by the RPA-ssDNA complex (Fig. 7*C*). However, the Rad51 filament was completely stable in the presence of either srs2 K41R (Fig. 7*D*) or srs2 K41A (Fig. 7*E*). Taken together, the results from the biochemical and electron microscopy analyses (Figs. 6 and 7) clearly indicated that disassembly of the Rad51 presynaptic filament by Srs2 requires the ATPase activity of the latter.

*Genetic Characterization of the srs2 K41A and srs2 K41R Mutant Alleles*—Previous studies (8, 9) of *SRS2* have highlighted the role of *SRS2* in attenuating Rad51-mediated recombination. We determined the effect of loss of Srs2 ATP hydrolysis on mitotic gene conversion, using two reporters that measure intra-chromosomal gene conversion between heteroalleles. As shown in Table I, both *srs2 K41A* and *srs2 K41R* elevated the gene conversion rates with both reporters. Interestingly, the hyperrecombination phenotype of two *srs2* mutants was even more pronounced than that of the *srs2* deletion mutant. Thus, the results show clearly that the antirecombination function of Srs2 requires the ATPase activity of this protein. Although the rate of gene conversion is increased in

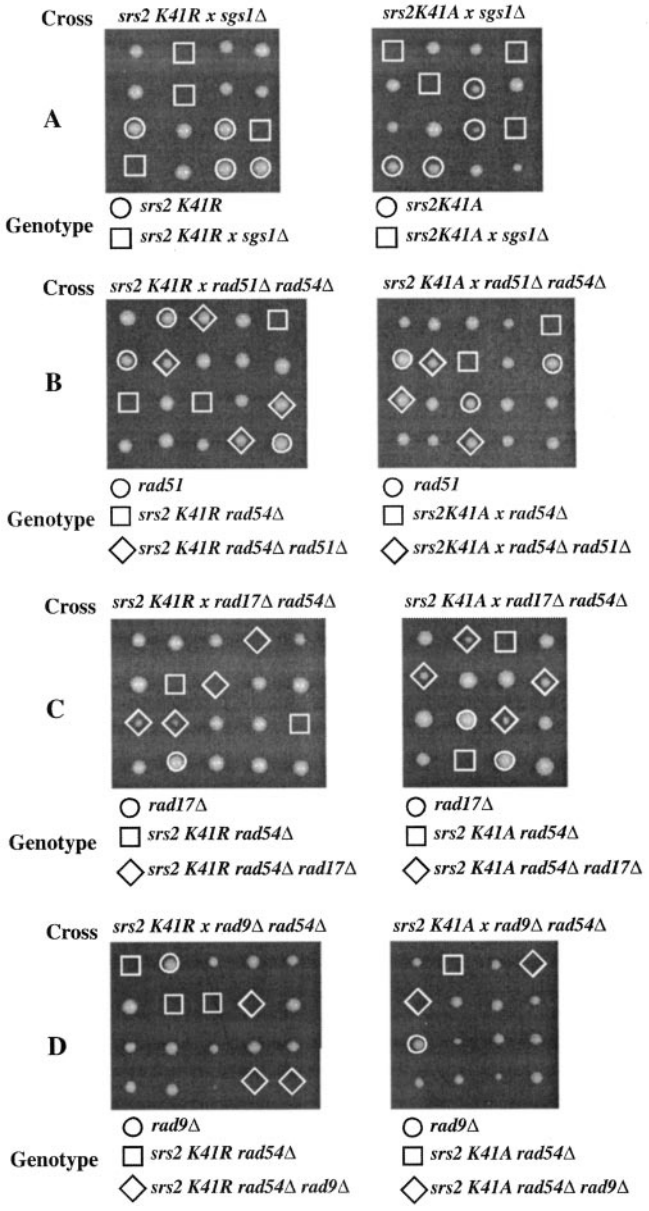


FIG. 9. **Synthetic lethal behavior of the *srs2 K41A* and *srs2 K41R* mutants.** Four or five tetrads from crosses indicated above each picture are shown. Synthetic lethality with the *sgs1*Δ mutation is shown in *A*. Synthetic lethality with the *rad54*Δ mutation is suppressed by loss of *RAD51* (*B*), partially suppressed by loss of the DNA damage checkpoint gene *RAD17* (*C*), and not suppressed by loss of the DNA damage checkpoint gene *RAD9* (*D*).

the *srs2* mutants, the spontaneous mutation rate measured for forward mutations at *CAN1* remains unchanged (Table II).

Mutants of *SRS2* are sensitive to MMS and other DNA damaging agents (8), and MMS sensitivity was actually used in our study to select transplacement segregants harboring the two *srs2* Walker mutant alleles (see "Materials and Methods"). The MMS sensitivity of the *srs2 K41A* and *srs2 K41R* strains is shown in Fig. 8. Both *srs2* mutants were sensitive in this assay, but the *srs2*Δ strain was significantly more sensitive than either of the two point mutants.

The *srs2*Δ mutation by itself is not lethal, but *srs2*Δ cells become inviable when *SGS1* or *RAD54* is also ablated (9, 11, 12). To determine the role of the Srs2 ATPase activity in these genetic interactions, we combined the *srs2 K41A* and *srs2 K41R* mutations with *sgs1*Δ or *rad54*Δ. The *srs2 K41A sgs1*Δ and *srs2 K41R sgs1*Δ double mutants are inviable or grow extremely

poorly (Fig. 9*A*), whereas the *srs2 K41A rad54*Δ and *srs2 K41R rad54*Δ double mutants are inviable (Fig. 9*B*). We checked the possible suppression of the *srs2 rad54*Δ lethality by *rad51*Δ, rad9Δ, or *rad17*Δ (8) by constructing the respective triple mutants. The lethality of *srs2 rad54*Δ is fully overcome by *rad51*Δ (Fig. 9*B*) and partially suppressed by *rad17*Δ (Fig. 9*C*), but *rad9*Δ was ineffective in this regard (Fig. 9*D*).

## DISCUSSION

To assess the role of ATP hydrolysis in Srs2 protein functions, we have constructed variants of this protein that harbor mutations in the Walker type A motif involved in ATP binding and hydrolysis. We have overexpressed the srs2 K41A and srs2 K41R proteins in *E. coli* and purified them to near homogeneity. Our biochemical analyses show that both of these mutant proteins retain DNA binding activity and the ability to interact with Rad51, but they are defective in ATP hydrolysis and lack DNA helicase activity. Both srs2 mutant proteins are unable to dissociate the Rad51 presynaptic filament and, accordingly, do not exert any inhibitory effect on Rad51-mediated homologous DNA pairing and strand exchange. The biochemical studies reported here thus establish the requirement for ATP hydrolysis in Srs2-mediated DNA unwinding and disassembly of the Rad51 presynaptic filament.

The results from our genetic studies provide support for the premise that ATP hydrolysis by Srs2 is needed to prevent untimely recombination, as the *srs2 K41A* and *srs2 K41R* mutants both exhibit a hyperrecombinational phenotype. Interestingly, the degree of hyperrecombination (measured as intrachromosomal gene conversion between heteroalleles) is even more pronounced in the srs2 point mutants than in the *srs2*Δ strain. In this regard, the two *srs2* Walker mutants resemble the *srs2–101* mutant described previously, which harbors the amino acid change of P39L, that is also significantly more hyperrecombinogenic than the *srs2*Δ mutant (9). These observations (Ref. 9 and this study) suggest that when Srs2 is absent, other non-recombinational pathways are used to repair spontaneous DNA damage, but when Srs2 protein is present but defective, it can interfere with these DNA repair pathways. Alternatively, or in addition, the *srs2* Walker mutants and the *srs2–101* mutant could induce DNA damage that is channeled into the homologous recombination pathway for repair, convert non-recombinogenic DNA lesions into recombinogenic ones, or enhance the activities of homologous recombination proteins. Because Srs2 is also important for the maximal activation of the S phase DNA damage checkpoint (18), it remains possible that the two *srs2* Walker mutants exert a positive influence on homologous recombination efficiency through its effect on checkpoint pathways (18). Further studies are needed to distinguish among these possibilities. That the *srs2 K41A* and *srs2 K41R* mutants do not behave exactly like the *srs2*Δ mutant is further attested by the observation that they are less sensitive to MMS than the latter. Just as in the case of *srs2*Δ (8, 9), we observed synthetic lethality of both *srs2* Walker mutants with either *rad54*Δ or *sgs1*Δ. We have also shown that the lethality of *srs2 K41A rad54*Δ and *srs2 K41R rad54*Δ can be overcome by deleting *RAD51* or *RAD17*.

Recently, reports from Haber and co-workers (20) and Kupiec and co-workers (19) showed that Srs2 is also needed for the repair of a site-specific double-strand break by synthesis-dependent single-strand annealing or double-ended synthesis-dependent single-strand annealing, the major pathway of gene conversion in mitotic yeast cells. In one of these published studies, the *srs2 K41A* allele was found to be defective in synthesis-dependent single-strand annealing (20). Likewise, the function of Srs2 in promoting adaptation or recovery from DNA damage checkpoint-mediated $G_2$/M arrest is reliant on its ATPase activity, as the *srs2 K41A* mutant is defective in this regard (17). We similarly expect the *srs2 K41R* mutant to be impaired in synthesis-dependent single-strand annealing and recovery/adaptation from DNA damage checkpoint-mediated $G_2$/M arrest. However, as alluded to above, whether or not the two srs2 Walker mutants retain S phase checkpoint function (18) will have to be determined experimentally.

We have demonstrated a physical interaction between Srs2 and Rad51 by the yeast two-hybrid system and also by biochemical means with purified proteins (14). We have suggested that the physical interaction between Rad51 and Srs2 may be germane for targeting the latter to chromosomal sites, *e.g.* ssDNA gaps created at stalled DNA replication forks, where Rad51 molecules are bound. However, it remains possible that the physical interaction noted (14) enables Srs2 to specifically displace Rad51 from ssDNA. The isolation of Rad51 and Srs2 mutants defective in complex formation will be necessary to address this issue.

## REFERENCES


1. Schmid, S. R., and Linder, P. (1992) *Mol. Microbiol.* **6,** 283–291
2. Howard, M. T., Neece, S. H., Matson, S. W., and Kreuzer, K. N. (1994) *Proc. Natl. Acad. Sci. U. S. A.* **91,** 12031–12035
3. Berneburg, M., and Lehmann, A. R. (2001) *Adv. Genet.* **43,** 71–102
4. Ellis, N. A., Groden, J., Ye, T. Z., Straughen, J., Lennon, D. J., Ciocci, S., Proytcheva, M., and German, J. (1995) *Cell* **83,** 655–666
5. Yu, C. E., Oshima, J., Fu, Y. H., Wijsman, E. M., Hisama, F., Alisch, R., Matthews, S., Nakura, J., Miki, T., Ouais, S., Martin, G. M., Mulligan, J., and Schellenberg, G. D. (1996) *Science* **272,** 258–262
6. Lawrence, C. W., and Christensen, R. B. (1979) *J. Bacteriol.* **139,** 866–876
7. Aguilera, A., and Klein, H. L. (1988) *Genetics* **119,** 779–790
8. Chanet, R., Heude, M., Adjiri, A., Maloisel, L., and Fabre, F. (1996) *Mol. Cell. Biol.* **16,** 4782–4789
9. Rong, L., Palladino, F., Aguilera, A., and Klein, H. L. (1991) *Genetics* **127,** 75–85
10. Lee, S. K., Johnson, R. E., Yu, S. L., Prakash, L., and Prakash, S. (1999) *Science* **286,** 2339–2342
11. Gangloff, S., Soustelle, C., and Fabre, F. (2000) *Nat. Genet.* **25,** 192–194
12. Klein, H. L. (2001) *Genetics* **157,** 557–565
13. Klein, H. L. (2000) *Nat. Genet.* **25,** 132–134
14. Krejci, L., Van Komen, S., Li, Y., Villemain, J., Reddy, M. S., Klein, H., Ellenberger, T., and Sung, P. (2003) *Nature* **423,** 305–309
15. Veaute, X., Jeusset, J., Soustelle, C., Kowalczykowski, S. C., Le Cam, E., and Fabre, F. (2003) *Nature* **423,** 309–312
16. Sung, P. (1994) *Science* **265,** 1241–1243
17. Vaze, M. B., Pellicioli, A., Lee, S. E., Ira, G., Liberi, G., Arbel-Eden, A., Foiani, M., and Haber, J. E. (2002) *Mol. Cell* **10,** 373–385
18. Liberi, G., Chiolo, I., Pellicioli, A., Lopes, M., Plevani, P., Muzi-Falconi, M., and Foiani, M. (2000) *EMBO J.* **19,** 5027–5038
19. Aylon, Y., Liefshitz, B., Bitan-Banin, G., and Kupiec, M. (2003) *Mol. Cell. Biol.* **23,** 1403–1417
20. Ira, G., Malkova, A., Liberi, G., Foiani, M., and Haber, J. E. (2003) *Cell* **115,** 401–411
21. Sherman, F. (1991) in *Guide to Yeast Genetics and Molecular Biology* (Guthrie, C., and Fink, G. R., eds) pp. 3–21, Academic Press, San Diego, CA
22. Thomas, B. J., and Rothstein, R. (1989) *Genetics* **123,** 725–738
23. Van Komen, S., Reddy, M. S., Krejci, L., Klein, H., and Sung, P. (2003) *J. Biol. Chem.* **278,** 44331–44337
24. Sugiyama, T., Zaitseva, E. M., and Kowalczykowski, S. C. (1997) *J. Biol. Chem.* **272,** 7940–7945
25. Krejci, L., Song, B., Bussen, W., Rothstein, R., Mortensen, U. H., and Sung, P. (2002) *J. Biol. Chem.* **277,** 40132–40141
26. Petukhova, G., Stratton, S., and Sung, P. (1998) *Nature* **393,** 91–94
27. Lea, D. E., and Coulson, C. A. (1949) *J. Genet.* **119,** 264–284
28. Sung, P., Higgins, D., Prakash, L., and Prakash, S. (1988) *EMBO J.* **7,** 3263–3269
29. Sung, P., and Stratton, S. A. (1996) *J. Biol. Chem.* **271,** 27983–27986
30. Sung, P., Krejci, L., Van Komen, S., and Sehorn, M. G. (2003) *J. Biol. Chem.* **278,** 42729–42732